Available online at www.sciencedirect.com
ScienceDirect
Scripta Materialia 57 (2007) 1145–1148
Scripta MATERIALIA
www.elsevier.com/locate/scriptamat

In situ high-energy X-ray diffraction study and quantitative phase analysis in the α + γ phase field of titanium aluminides

LaReine A. Yeoh,[a,*] Klaus-Dieter Liss,[a] Arno Bartels,[b] Harald Chladil,[c] Maxim Avdeev,[a] Helmut Clemens,[c] Rainer Gerling[d] and Thomas Buslaps[e]

[a] *Bragg Institute, Australian Nuclear Science and Technology Organization, Private Mail Bag 1, Menai NSW 2234, Australia*
[b] *Department of Materials Science and Technology, Technical University of Hamburg-Harburg, Eissendorferstrasse 40, D-21073 Hamburg, Germany*
[c] *Department of Physical Metallurgy and Materials Testing, Montanuniversität, Franz-Josef-Strasse 18, A-8700 Leoben, Austria*
[d] *Institute for Materials Research, GKSS-Research Centre, Max-Planck-Strasse 1, D-21502 Geesthacht, Germany*
[e] *European Synchrotron Radiation Facility, B.P. 220, F-38043 Grenoble Cedex, France*

Received 16 June 2007; revised 6 August 2007; accepted 7 August 2007
Available online 21 September 2007

Quantitative atomic structure and phase analysis in the titanium aluminide intermetallic system of composition Ti–45Al–7.5Nb–0.5C (at.%) was conducted in situ by use of high-energy X-ray diffraction from a synchrotron and evaluated using the Rietveld method, implementing a model for atomic order in the α-phase which describes the order to disorder transition $\alpha_2 \rightarrow \alpha$ at the eutectoid temperature. The order parameter exhibits unexpected behavior and is entangled with the competition of different kinetic processes.

Keywords: Titanium aluminides; Intermetallic compounds; Order–disorder phenomena; Phase transformation kinetics; Synchrotron radiation

The properties of intermetallic γ-based TiAl alloys render them very desirable for high-temperature applications in the automotive and aerospace industries [1]. Understanding an alloy's phase constituents and behavior over transition temperatures is important for optimizing the mechanical properties of the material. In classical physical metallurgy, microstructural and atomic arrangements from heat-treated samples are studied ex situ after being quenched from a high temperature state, whilst the temperatures of phase transitions and reactions are often obtained from differential scanning calorimetric measurements. Although in situ diffraction studies have been reported previously [2,3], very little is known about the observed details behind phase transitions. With the introduction of high-energy X-ray diffraction, however, information can be gathered in real time and in situ from the bulk of a material [4–7]. Such data sets are extremely rich in information and now shed light upon the characteristic phase evolution occurring some distance from the transition temperature. The present study follows the competition between phases within the α + γ two-phase field (Fig. 1), of a high niobium-containing titanium aluminide alloy, which is one of the most important interplays in the processing of these intermetallic materials. The multitude of microstructures in this phase field, ranging from globular to duplex and lamellar [1], highlights the need for quantitative in situ information, both at and far from the thermodynamic equilibrium, as investigated in this work.

The investigated Ti–45Al–7.5Nb–0.5C sample (composition in at.%) is part of a series [8] of different high Nb-containing γ-TiAl-based alloys which have been produced using a powder metallurgical approach, guaranteeing a homogeneous chemical distribution of the constituent elements. Pre-alloyed powder was produced by means of gas atomization in the PIGA (plasma melting induction guiding gas atomization) facility at the GKSS Research Center [9]. Powder of particle size <180 μm was placed in a titanium can, which then was degassed, welded and subsequently hot-isostatically pressed (HIP) at 200 MPa for 2 h at 1553 K. Chemical analysis indicated that the compositions of both the alloy powder and the HIP material matched the nominal

* Corresponding author. E-mail: lareine.yeoh@gmail.com

1359-6462/$ - see front matter
doi:10.1016/j.scriptamat.2007.08.021

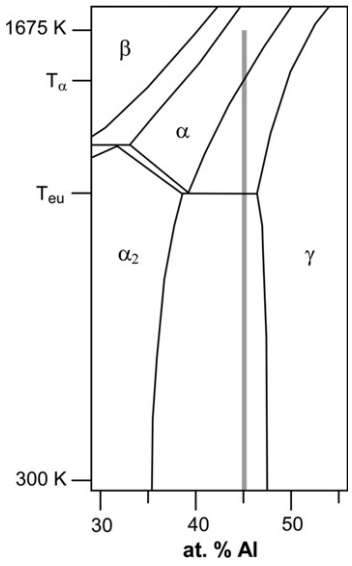

Figure 1. Quasi-binary phase diagram, based on Ti–Al from Ref. [17], showing the relevant region of interest. The scale to the left is not drawn linearly and indicates only schematically the heating range and transition markers for the used composition represented by the vertical gray line. It should be noted that alloying additions such as Nb and C have a marked influence on the shape of the phase diagram (see e.g. [8]).

compositions within the experimental error. After HIP, the content of oxygen and nitrogen was analyzed to be 450 and 50 mass ppm, respectively. During HIP a duplex microstructure is formed which consists of globular γ-TiAl/α_2-Ti_3Al grains. The average grain size is about 15 μm [10].

High-energy X-rays employing a two-dimensional detector were used to conduct diffraction studies at the ID15B beamline at the ESRF in Grenoble [4,5]. A furnace was used to control the temperature with an input of helium flow to reduce oxidation [8]. The Ti–45Al–7.5Nb–0.5C sample in the as-HIPed condition was ramped from room temperature up to 1375 K at 5 K min^{-1} before the ramp was lowered down to 2 K min^{-1}. Once the temperature reached 1675 K, it was maintained for 5 min and then subsequently cooled down to room temperature at 5 K min^{-1}. Although the sample was in direct contact with a regular type-S thermocouple, temperature readings on the ramp were not particularly accurate and required re-calibration to the α-transus temperature of the Ti–45Al–7.5Nb–0.5C alloy obtained via differential scanning calorimetry on a sample from the same batch [8].

The X-ray energy, wave number, detector distance and pixel size of the beamline were calibrated to 89.05 keV, 45.12 $Å^{-1}$, 1146 mm and 0.150 mm, respectively. The software package dataRring was developed at ANSTO [11] on the SCILAB platform [12] to reduce the two-dimensional diffraction patterns into one-dimensional diffractograms with a regular 2θ scaling as necessary to be converted into GSAS format for quantitative phase analysis [13,14].

Batch Rietveld refinement was conducted in the $\alpha + \gamma$ phase field upon heating to the alpha transus temperature $T_\alpha = 1565$ K, using a model that describes the coexistence of both phases, namely hexagonal α_2/α-Ti_3Al and tetragonal γ-TiAl.

The hexagonal phase was modeled as α_2 throughout the entire temperature range, taking into account the atomic disorder within the unit cell itself. It treats the α_2 and α phases as a single phase (space group $P6_3/mmc$, $a \sim 5.8$ Å, $c \sim 4.7$ Å), with the α phase being a fully disordered state of the α_2 phase. There is also a constraint on the total site occupancy ratio, which is set to 1. This model does not include the chemical disorder that is introduced by the deviation from stoichiometry. There is a continuous exchange of atoms between the γ- and the α-phase depending on the position in the phase diagram and thus a change of the composition of the α-phase takes place as temperature varies. This additional parameter was not included in the Rietveld model and thus chemical disorder will have to be added to the results obtained from the fit, which has not been further considered here. We interpret the site occupancies as 100% for the maximal order that the chemical composition of the phase will allow.

Further, the Nb atoms were treated as being evenly distributed across the Ti sites, and both kinds of atoms could not be distinguished in the model. Without doubt, the Nb content influences all the evaluated data, including the phase fraction, the lattice parameters and the eutectoid temperature, T_{eu}. It is known that the carbon content stabilizes, and leads to a higher c/a ratio of, the α_2-phase [8], but we did not aim to specify these influences in the present work, as we would have needed comparable data without these elements.

Figure 2a and b shows the integrated intensity values of the γ-0 0 1 and α_2-1 0 1 reflections as a function of temperature for both heating and cooling. Upon heating, the α_2-phase drops considerably at the $\alpha_2 \rightarrow \alpha$ transition, which occurs at $T_{eu} = 1476$ K, while the γ-0 0 1 intensity drop has a kink in its slope and decreases continuously until $T_\alpha = 1565$ K. In contrast, the nucleation of the γ-phase is delayed upon cooling and appears at 1518 K, resulting in an undercooling of −47 K. Undercooling effects of this transition were observed at numerous occasions [15] and stem from the small difference in the Gibbs free energy of both phases at T_α. It increases at lower temperatures, driving the probability for nucleation and then the growth of the appearing γ-phase. The α_2-1 0 1 reflection, however, reappears at a higher temperature, 1539 K, which is +63 K earlier than expected at T_{eu}, which itself was obtained from the heating section and the complementary differential scanning calorimetry measurements. It shows a change in the slope at T_{eu}.

With the actual sets of data, an explanation for the early observation of ordering of α to α_2 can only be speculative, and may be related to the changes in local chemistry and α_2 stabilizing oxygen content which was taken up during the experiment. Comparison of the behavior of the intensities also shows that the phase fractions γ/α are higher on heating than on cooling. However, for this paper, the following quantitative analysis will concentrate on the heating section only.

The quantitative Rietveld results are presented in Figure 2c–f for the γ- and α-phase fractions, the c/a ratio of lattice parameters and site occupancies of the α_2-phase and the c/a ratio of the γ-phase, respectively.

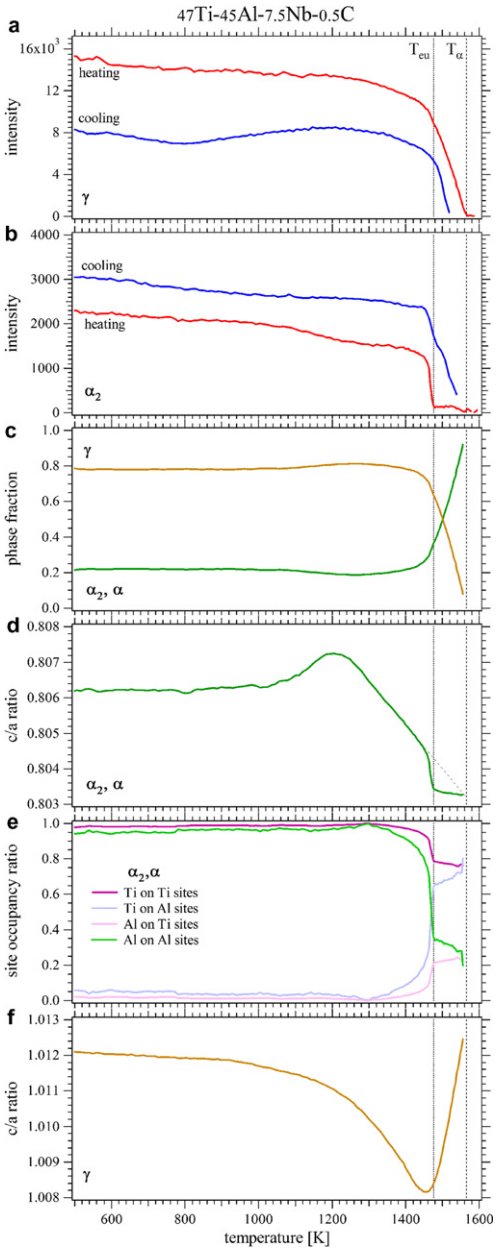

Figure 2. Temperature dependencies of reflections and Rietveld results. (a) peak intensity of the γ-0 0 1 reflection upon heating (upper) and cooling (lower curve); (b) α_2-1 0 1 reflection upon heating (lower) and cooling (upper curve); (c) γ/α-phase fractions; (d) *c*/*a* ratio and (e) site occupancies in the α_2-phase; (f) *c*/*a* ratio of the γ-phase. A starting material Ti–45Al–7.5Nb–0.5C with duplex microstructure was used. The dotted lines indicate T_{eu} and T_α.

It can be seen from Figure 2c that the system starts with a phase fraction composition of 78% γ and 22% α_2, which increases to 81% γ at 1280 K, before the γ transforms into α and vanishes at T_α. We attribute this initial raise in γ to a residual, non-equilibrium state of the phase composition in the starting material. Although furnace cooling is used after the HIP process, a higher α_2-phase fraction is retained at room temperature in contrast to the expected values for thermodynamic equilibrium for which an infinitely small cooling rate is required. Around 1050 K a small raise in γ -fraction can be seen from Figure 2c. It is assumed that at this temperature the constituting atoms become mobile enough to undergo the phase transition $\alpha_2 \rightarrow \gamma$ [16]. At higher temperatures, the $\gamma \rightarrow \alpha_2$ transition prevails and increases rapidly at 1460 K.

The qualitative behavior of the *c*/*a* ratio in the α_2-phase is similar, namely starting with a relatively high value of 0.8062, which increases above 1050 K to a peak value of 0.8073 at 1205 K before continuing to decrease to 0.8033 towards T_α, where the phase undergoes an order → disorder transition. The change in composition in the α_2-phase dominates the behavior of the *c*/*a* ratio. The system starts with a small oversaturation of the α_2-phase due to the production history (HIP and cooling). The mobility of atoms becomes high enough above 1050 K that the concentrations of (Ti, Nb) and Al tend towards equilibrium. The *c*/*a* ratio starts to increase accordingly due to an increase in the Ti-content of the α_2-phase and a small decrease in the phase fraction. Around 1200 K the equilibrium of phases and phase composition is reached, and the process of increasing chemical disorder can be followed upon further heating, combined with a steady decrease in the Ti-content of the α_2-phase resulting in the observed linear decrease in *c*/*a*. It is observed that a linear extrapolation of the *c*/*a* decrease up to T_α coincides with the *c*/*a*-ratio of the disordered α-phase.

The site occupancy curves from Figure 2e represent the average amount of the chemical disorder within the site occupancies of the Ti and Al atoms for the α_2-phase, with both curves for one type of site having a total site occupancy of 100%. Due to the slow cooling rate during the manufacture of the sample, the material initially starts off in near-thermodynamic equilibrium with a fairly low amount of atomic disorder. The order in the α_2-phase at room temperature is high, with 94.1% of Al atoms on Al lattice sites and 97.9% of Ti (+Nb) atoms on Ti lattice sites. Thus 5.9% of Ti (+Nb) and 2.1% of Al atoms can be said to be in an atomically disordered state. The Ti:Al ratio of the disordered part is 2.8:1, which is close to the expected stochiometric value of 3:1 for Ti_3Al.

However, as the temperature approaches T_α, the amount of disorder slowly increases until the phase transition is reached, at which point there is a sudden jump in the occupancies of the atoms, defining the phase transition at T_{eu}. After the phase transition, the amount of Ti atoms sitting on both the Ti and Al sites tends towards ~75%, and the amount of Al atoms sitting there tends towards ~25%, again following the initial stoichiometric ratio of Ti_3Al closely.

A closer inspection of the occupancy behavior over the whole heating ramp reveals a tendency towards 100% order at 1300 K. This is consistent with the behavior of the phase fraction and *c*/*a* ratio of the α_2-phase, where disorder, initially frozen into the system during the production process, disappears and atoms become mobile. However, the temperatures at which these behaviors peak differ, with the *c*/*a* ratio peaking first, then the phase fraction followed by the site occupancy. From this, it seems that the *c*/*a* ratio is not solely determined by atomic order, but is further biased by another process which decreases it linearly with increasing temperature between 1250 and 1440 K. It should be noted

that the ratio loses this linearity just before T_{eu} is reached, though the final point at T_α lies once again on the extrapolated straight line.

The c/a behavior of the γ-phase is shown in Figure 2f as a function of temperature. It first decreases continuously until the onset of the $\alpha_2 \rightarrow \alpha$ disorder transition at 1460 K, then increases again rapidly with the ongoing transition from $\gamma \rightarrow \alpha$, reaching its maximum value at T_α. The face-centered tetragonal structure of the γ-phase distinguishes the crystallographic **c** direction by alternating layers of Ti and Al atoms from **a** staggered by planes that each contain both atom types. Thus, if the lattice was fully disordered, there would be no distinction between the directions and the lattice would be cubic. In a thought experiment, the lattice can be described by a cubic and a tetragonal component, which is related to the order of the phase. The observed behavior is then related to the chemical disorder, which is given in thermodynamic equilibrium by the phase line between the $(\alpha_{(2)} + \gamma)$ and the γ-phase fields [17]. As such, the observed behavior of $c/a|_\gamma$ can be interpreted as follows: $c/a|_\gamma$ shows a small linear decrease up to 900 K, and this describes the anisotropy of thermal expansion of the γ-phase. In this temperature range $c/a|_\alpha$ is nearly constant. Above this temperature, the rate of decrease of $c/a|_\gamma$ is more than linear until T_{eu} is reached. This is predominantly caused by the decrease of the Al-content in the γ-phase and the induced chemical disorder. In accordance with the phase diagram [17], the lowest possible Al-content in the γ-phase is reached at T_{eu} and, therefore, at the lowest $c/a|_\gamma$-ratio. Both values increase again at higher temperatures. The smaller slope of the respective phase line is consistent with the faster evolution above compared with below T_{eu}.

The phase compositions and crystallographic lattice parameters in the $\alpha_{(2)} + \gamma$ phase field of titanium aluminides depend on order and disorder within the atomic structure and on the initial deviation from the thermodynamic equilibrium during manufacture. The resulting phenomena manifest themselves as anomalies in behavior with respect to temperature. The study reveals a series of new results, such as the $\alpha_2 \rightarrow \alpha$ transition and its corresponding precursor behaviors and aftereffects, which can be extrapolated to the α-transus temperature. During the decrease in temperature, undercooling occurs and the appearance of the γ-phase is delayed, whilst the α-phase orders earlier than expected, which may be related to the interplay of the atomic structures and changes in local chemistry of the phases.

The Australian writers acknowledge financial support from the Access to Major Research Facilities Programme, which is a component of the International Science Linkages Programme established under the Australian Government's innovation statement, Backing Australia's Ability. The Austrian authors thank the Styrian Materials Cluster for continuous support, and B.A. and G.E. acknowledge the support of the German Science Foundation, DFG (projects BA 1147/1 and GE 1115/2).

[1] H. Kestler, H. Clemens, in: M. Peters, C. Leyens (Eds.), Titanium and Titanium Alloys, Wiley-VCH, Weinheim, 2003, pp. 351–392.
[2] R.D. Shull, J.P. Cline, High Temperature Science 26 (1989) 95–117.
[3] T. Novoselova, S. Malinov, W. Sha, A. Zhecheva, Materials Science and Engineering A – Structural Materials Properties Microstructure and Processing 371 (2004) 103–112.
[4] K.-D. Liss, A. Bartels, A. Schreyer, H. Clemens, Textures and Microstructures 35 (3/4) (2003) 219–252.
[5] K.-D. Liss, A. Bartels, H. Clemens, S. Bystrzanowski, A. Stark, T. Buslaps, F.-P. Schimansky, R. Gerling, C. Scheu, A. Schreyer, Acta Materialia 54 (14) (2006) 3721–3735.
[6] K.-D. Liss, A. Bartels, H. Clemens, S. Bystrzanowski, A. Stark, T. Buslaps, F.-P. Schimansky, R. Gerling, A. Schreyer, Materials Science Forum 539–543 (2007) 1519–1524.
[7] K.-D. Liss, H. Clemens, A. Bartels, A. Stark, T. Buslaps, Advanced Intermetallic-Based Alloys – Mater. Res. Soc. Symp. Proc. 980, Warrandale, PA (2007) 0980-II05-07.
[8] H.F. Chladil, H. Clemens, G.A. Zickler, M. Takeyama, E. Kozeschnik, A. Bartels, T. Buslaps, R. Gerling, S. Kremmer, L.A. Yeoh, K.-D. Liss, International Journal of Materials (Zeitschrift für Metallkunde), in press.
[9] R. Gerling, H. Clemens, F.P. Schimansky, Advanced Engineering Materials 6 (2004) 23–38.
[10] H.F. Chladil, H. Clemens, H. Leitner, A. Bartels, R. Gerling, F.P. Schimansky, S. Kremmer, Intermetallics 14 (2006) 1194–1198.
[11] dataRring. LaReine Yeoh, Klaus-Dieter Liss, Lucas Heights, Australia, Bragg Institute, ANSTO (2006).
[12] SCILAB©. INRIA ENPC. 1989–2005, <http://www.scilab.org>.
[13] A.C. Larson and R.B. Von Dreele, General Structure Analysis System (GSAS), Los Alamos National Laboratory Report LAUR 86–748 (2000).
[14] B.H. Toby, Journal of Applied Crystallography 34 (2001) 210–213.
[15] A. Bartels, S. Bystrzanowski, H. Chladil, H. Leitner, H. Clemens, R. Gerling, F.-P. Schimansky, Materials Research Symposium Proceedings 842 (2005) 5.48.1–5.48.6.
[16] W. Schillinger, H. Clemens, G. Dehm, A. Bartels, Intermetallics 10 (2002) 459–466.
[17] J.C. Schuster, M. Palm, Journal of Phase Equilibria and Diffusion 27 (2006) 255–277.